Image Cover Sheet

CLASSIFICATION	SYSTEM NUMBER
UNCLASSIFIED	49783

TITLE

LOW DOPPLER TARGET DETECTION IN GROUND CLUTTER

System Number:

Patron Number:

Requester:

Notes:

DSIS Use only:

Deliver to:

COMMUNICATIONS RESEARCH CENTRE

DEPARTMENT OF COMMUNICATIONS
CANADA

LOW DOPPLER TARGET DETECTION IN GROUND CLUTTER

by

John S. Bird

(Radar and Communications Technology Branch)

CRC REPORT NO. 1397

November 1985
OTTAWA

This work was sponsored by the Department of National Defence, Research and Development Branch under Project No. 33C69.

TABLE OF CONTENTS

The key to the utility of coherent thresholding lies in the very nature of the clutter returns. These returns must be coherent over the long term (minutes, hours, days, etc.). It is the purpose of this report to demonstrate that a large portion of ground clutter does possess this long term coherency and to use this characteristic of the clutter to establish the merits of coherent clutter processing. Since we are primarily concerned with detecting low Doppler targets the comparison will be between the adaptive and coherent thresholding techniques.

In addition it will be shown that coherent clutter processing can be used to identify or differentiate certain target and/or clutter types from a background of heavy ground clutter.

Coherent thresholding was first presented in the context of a coherent clutter map in 1982 [6]. Further evidence of the viability of the technique was presented in 1984 [7]. This report combines these results, presented in more detail, with new experimental evidence and an extention to multiple dwells. The theoretical and experimental results are presented in the operational context of an adaptive ground-based phased-array surveillance radar.

This report is divided into 6 sections, the first of which is the introduction. The second section examines the coherent nature of ground clutter and its statistical representation in the phase plane. The third section describes the effect of coherent clutter on various detection schemes and defines the coherent-to-diffuse power ratio, CDR, as a measure for comparison. Experimental evidence to support the suggested model for ground clutter and to describe the extent to which the model holds for different terrain types, seasons, wind speeds and times of day is given in section 4. In section 5 experimental clutter results are used to demonstrate the detectability of low-Doppler targets in real ground clutter and the merits of a coherent clutter map. The final section concludes the discussion by summarizing the main result and suggesting direction for further work.

2.0 CLUTTER AND TARGET RETURNS

2.1 Receiving System

The receiving system under consideration is shown in Figure 1. It consists of a coherent receiver followed by a base-band zero-Doppler filter. (Other Doppler filters are used to detect targets at higher Doppler frequencies but are not shown.)

The output of the zero-Doppler filter consists of the coherent sum of K returns and may be represented in the phase plane as a single point. The outputs for several groups of K returns plotted in the phase plane is a scatter plot of zero-Doppler clutter returns. This scatter plot characterizes the probability distribution of the interference which the target must compete against for detection. Several assumptions about this clutter distribution will be made and supported by experimental evidence.

2.2 Phase Plane Description of Ground Clutter

Ground clutter as seen by a step-scan radar consists of a coherent component and a diffuse component the relative powers of which depend on the nature of the clutter. Figure 2 illustrates this by showing 50 returns, plotted in the phase plane, for a patch of clutter consisting of a small metal research tower and bush. The individual returns were separated by 8 seconds with the complete scatter plot representing 6.67 minutes of data.

These returns are tightly grouped in the phase plane about an average amplitude and phase. The amplitude of the coherent component of the clutter is defined as

$$C \triangleq (u_I^2 + u_Q^2)^{\frac{1}{2}} \tag{1}$$

where

$$u_I = \frac{1}{N} \sum_{n=1}^{N} I(n) \tag{2}$$

$$u_Q = \frac{1}{N} \sum_{n=1}^{N} Q(n) \tag{3}$$

where I(n) and Q(n) are the in-phase and quadrature components of the n^{th} output of the zero-Doppler filter. For Figure 2 each point represents a single return as the length, K, for the filter was 1. The phase of the coherent component of the clutter is defined as

$$\theta \triangleq \arctan\left(\frac{u_Q}{u_I}\right) \tag{4}$$

The amplitude of the diffuse component is defined from the variation about the mean clutter point as

$$D \triangleq (\sigma_I^2 + \sigma_Q^2)^{\frac{1}{2}} \tag{5}$$

where

$$\sigma_I^2 = \frac{1}{N-1} \sum_{n=1}^{N} (I(n)-u_I)^2 \tag{6}$$

$$\sigma_Q^2 = \frac{1}{N-1} \sum_{n=1}^{N} (Q(n)-u_Q)^2 \tag{7}$$

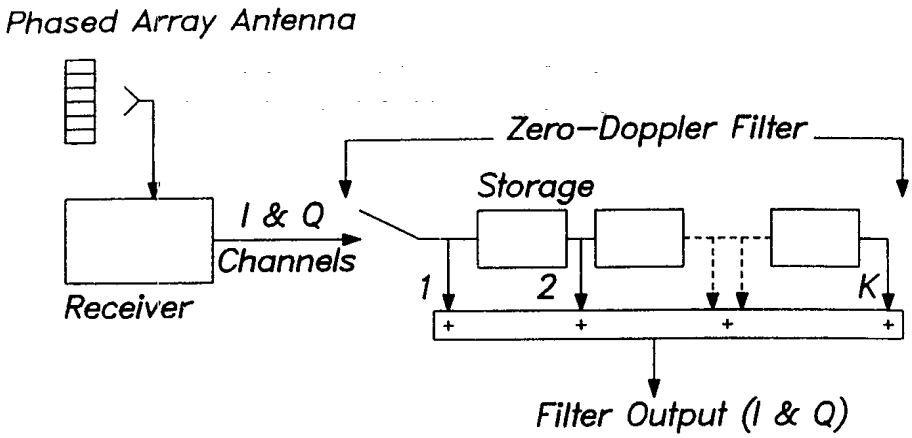

Fig. 1 Radar receving system.

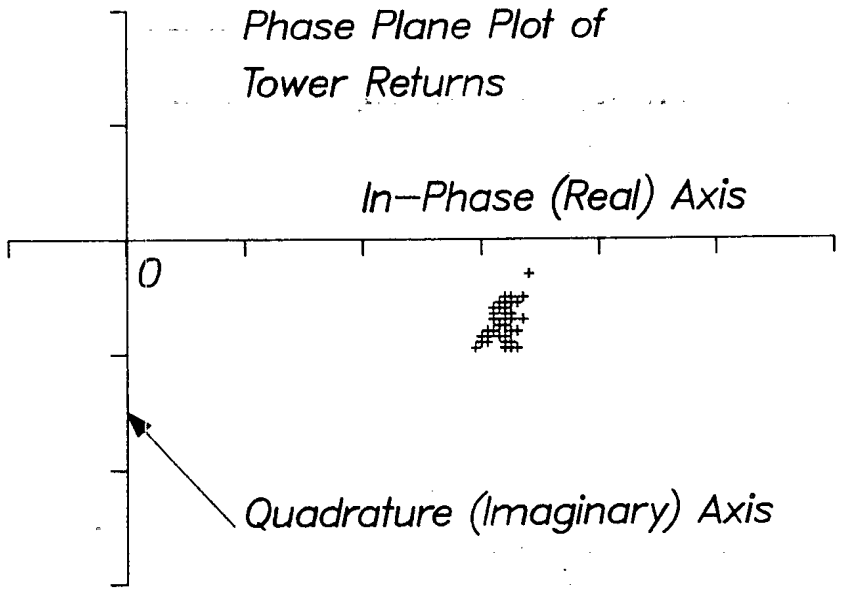

Fig. 2 Phase plane plot of 50 returns from a metal tower and bush.

The diffuse component of the clutter is also assumed to contain a system noise component since the two cannot be separated. Therefore in areas where the clutter returns are very small or almost entirely coherent, a large part of the diffuse component will be system noise. On the other hand, when the diffuse component of the clutter is large, the contribution due to system noise will be negligible.

The coherent-to-diffuse power ratio is defined as

$$\text{CDR} \triangleq \frac{C^2}{D^2} = \frac{u_I^2 + u_Q^2}{\sigma_I^2 + \sigma_I^2} \tag{8}$$

For the data shown in Figure 2 the CDR was 24 dB indicating that the power associated with the coherent component of the clutter was 24 dB larger than that associated with the diffuse component. The CDR is an important measure in determining how effective coherent thresholding techniques will be in combating clutter.

3.0 TARGET DETECTION AND IDENTIFICATION

In this section the concept of clutter returns consisting of a coherent as well as a diffuse component is used to develop coherent thresholding techniques that can significantly increase low-Doppler target detectability. Also it is shown how certain targets can be identified by exploiting differences from surrounding clutter.

3.1 Target Detection

In conventional radars it is standard practice to use a measure of the power of clutter returns as a parameter to set detection thresholds. Depending on how close the actual clutter distribution is to the assumed distribution, the results of such a procedure can be good or disastrous. A probability distribution that is often used to describe the amplitude of clutter returns is the Rayleigh distribution. This distribution describes the amplitude of a complex variable whose real and imaginary components are independent identically distributed Gaussian random variables. We will use this distribution to describe the diffuse component of the clutter and show how a coherent component in the clutter drastically affects the performance of detection schemes that make the diffuse assumption for the complete clutter return.

The performance of three thresholding techniques will be compared. The first technique, which is used in many radars, assumes that the entire clutter return is diffuse (Gaussian in-phase and quadrature components) and sets the threshold accordingly. The second technique makes no assumption about the distribution but dynamically adjusts the threshold until the desired probability of false alarm is attained. The third technique recognizes the possibility of a coherent component in the clutter and establishes a threshold around the average clutter vector in the phase plane. This final technique is referred to as a coherent thresholding.

In making the above comparisons it is assumed that the target amplitude distribution is Rayleigh and that the target return is independent from sample to sample. This assumption means that the target return simply augments the diffuse component of the clutter at the output of the zero-Doppler filter. Comparisons will be made on the basis of the probability of detection with CDR and signal-to-clutter ratios being defined at the filter output. Where K returns are combined in the filter the single return coherent-to-diffuse ratio, CDR_S, is

$$CDR_S = \frac{CDR}{K} \tag{9}$$

where it is assumed that the diffuse components of the returns are independent.

3.1.1 Thresholding Schemes

3.1.1.1 Conventional Thresholding

Conventional thresholding assumes that the amplitude of the total clutter return is Rayleigh distributed.

$$p(r) = \frac{2r}{P^2} \exp\left(\frac{-r^2}{P^2}\right) \tag{10}$$

where r is the amplitude and P^2 is the returned clutter power. Therefore the threshold required to maintain a certain probability of false alarm is

$$T_G = \left(P^2 \ln\left(\frac{1}{P_F}\right)\right)^{\frac{1}{2}} \tag{11}$$

where T_G is the threshold (the subscript G signifies that the clutter signal distribution is assumed to be Gaussian) and P_F is the probability of false alarm. If the clutter return is made up of a coherent and diffuse component the threshold T_G becomes

$$T_G = \left((C^2 + D^2) \ln\left(\frac{1}{P_F}\right)\right)^{\frac{1}{2}} \tag{12}$$

and the true probability of false alarm becomes the integral of a Ricean distribution

$$P_{FG} = \int_{T_G}^{\infty} \frac{2r}{D^2} \exp\left(\frac{-(C^2 + r^2)}{D^2}\right) I_0\left(\frac{2Cr}{D^2}\right) dr \tag{13}$$

where $I_0(\cdot)$ is the modified Bessel function of order zero and the subscript G indicates that this is not the design P_F.

$$P_{DC} = \exp\left(\frac{- T_C^2}{(S^2 + D^2)} \right) \tag{17}$$

3.1.2 Performance Comparisons

3.1.2.1 Single Sample Detection

It is shown in the appendix that the signal-to-interference ratio gain achieved by using one threshold technique over another can be attained by equating the appropriate expressions for probability of detection by scaling the target power. The general expression for this gain is quite complicated and therefore it is difficult to relate it to the clutter paramters C and D. Considerable simplification is achieved under a large signal assumption for which the gain becomes the ratio of the squares of the two thresholds. Although this assumption is not strictly true for our analysis, the gain so obtained is a good estimate of the actual gain for signal-to-diffuse ratios as small as those required for $P_{DC} = 0.8$. Therefore the signal-to-interference power gain achieved (this is equivalent to a signal-to-noise ratio gain) by using coherent thresholding over conventional thresholding is

$$SIR_G \simeq \frac{T_G^2}{T_C^2} = CDR + 1 \tag{18}$$

where SIR_G is the signal-to-interference power gain and CDR is the coherent-to-diffuse power ratio defined in (8). The gain for using coherent thresholding rather than adaptive thresholding is not easily determined because there is no explicit expression for T_A. However, from the detection curves to follow it will be seen that the gain is "approximately" one-half (in decibels) of that shown in (18).

To illustrate the significance of this gain consider again Figure 2. For this resolution cell the CDR is 24 dB and therefore the SIR_G is approximately 24 dB as well since the linear addition of one is insignificant. A target that is just detectable with the coherent threshold would have to have a 24 dB larger cross section to be detectable using a conventional threshold and 12 dB larger using an adaptive threshold.

How this large detection gain is achieved is illustrated in Figure 3. For a single sample from the zero-Doppler filter the threshold T_G is equivalent to establishing a circular contour in the phase plane and declaring a target present if the return is outside this contour. Figure

3a shows the circular contour and corresponding decision regions. If the clutter possesses a coherent and diffuse component as shown by the offset circle, a target which is random in phase is more likely to be detected with the offset coherent threshold shown in 3b than the centred threshold of in Figure 3a. The centred threshold must be large enough to encompass the entire coherent component no matter how small the diffuse component otherwise the false alarm probability will be large. The offset threshold, however, need only encompass the diffuse component.

Probability of detection curves for a design P_F of 10^{-4} and two values of CDR are shown in Figure 4. The same curve is shown for the coherent threshold because its performance is independent of the size of the coherent clutter component. Coherent thresholding has a gain of CDR+1 over conventional thresholding and approximately one-half that over adaptive thresholding. It should be noted that as the coherent component decreases all three thresholds coincide and their performances are identical.

These curves show the performance for a single sample at the output of the zero Doppler filter. If the filter integrates K returns, the SCR and CDR must be scaled to get the single return ratios as outlined in equation (9).

3.1.2.2 Multiple Sample Detection

Multiple sample detection involves noncoherently integrating M samples from the zero-Doppler filter with each sample composed of the coherent sum of K different returns. A square-law detector is assumed. Coherent thresholding is accomplished by substracting a coherent estimate of the clutter mean from the sample before it enters the square-law detector. Therefore the performances of the conventional and adaptive thresholds are described using the noncentral chi-squared distribution with 2M degrees of freedom and that of the coherent threshold with the central chi-squared distribution, respectively. Probabilities of false alarm and detection are determined through the use of the generalized Q function [8].

Figure 5 shows the performance of the three thresholds for M=10 and two values of CDR. The gain for using coherent thresholding over conventional is approximately equal to the CDR+1, as is shown in the Appendix, for a large signal assumption and M=1. This estimate of the gain was found to be good for all of the cases calculated using different values of M and signal-to-clutter ratios such that P_D = .8 for the coherent threshold.

3.2 Target Identification

The essence of target identification is to observe the returns from a target and those from surrounding clutter objects and be able to tell the difference. If the target is not moving and is immersed in a "sea" of large stationary clutter objects this is indeed a very difficult

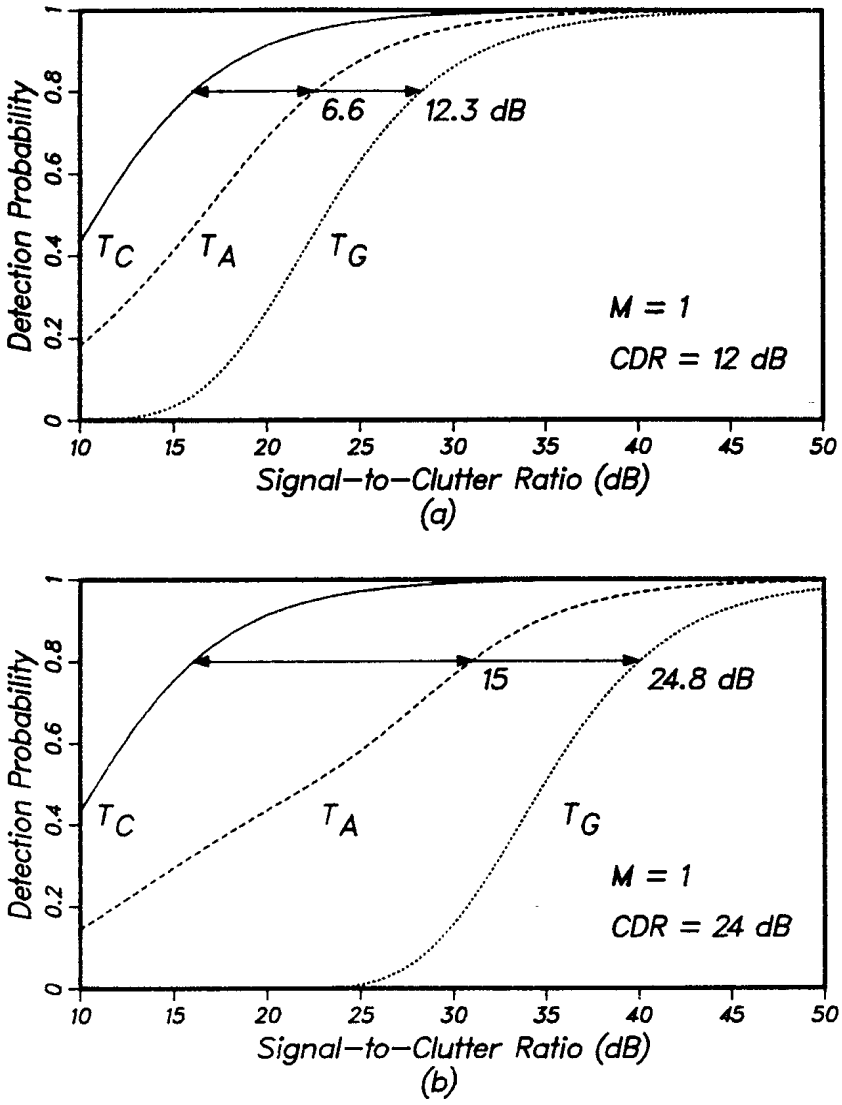

Fig. 4 Single sample probability of detection curves for the three thresholds for CDR's equal to 12 and 24 dB, and $P_F=10^{-4}$.

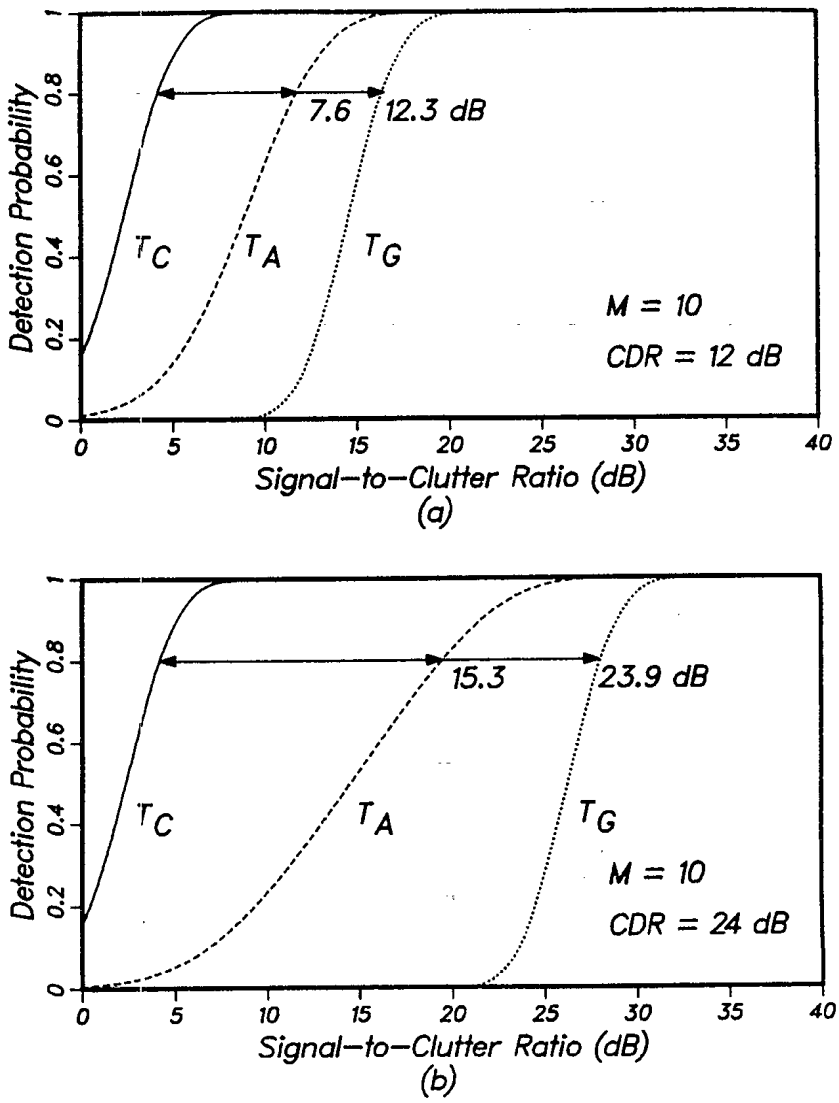

Fig. 5 M sample probability of detection curves for the three thresholds for CDR's equal to 12 and 24 dB and $P_F=10^{-4}$.

problem. To illustrate how coherent clutter processing can be used in some situations to solve this problem, consider a stationary man-made structure located in bush type terrain. As was already stated clutter returns from bush tend to be diffuse (how much so will be discussed in the next section), but the returns from the man-made structure tend to be coherent. Therefore by calculating the CDR as described in (8) for each range cell as the radar searches the terrain it is possible to identify the cell with the man-made structure as that with an abnormally large CDR. This is possible even though the total return from the structure is much smaller than the surrounding returns. Similarly, it is possible to detect the presence of new objects in a range cell or changes in a structure by observing shifts in the coherent mean of the returns.

Figure 6 shows an example of radar clutter returns as a function of range. The solid line represents the coherent target cross section and the dotted line the diffuse target cross section. It is clear from the profile that the object causing the return from point "A" is different in nature from the surrounding objects. This object is a metal tower which is surrounded by bush. Although the tower, in terms of total returned power, does not stand out as anything different it is clearly separated from the background clutter when coherent decomposition is used.

4.0 EXPERIMENTAL EVIDENCE OF APPLICABILITY

Since the merits of coherent clutter decomposition for target detection and identification depend on the nature of the clutter being observed, a year-long clutter measurement program with this application in mind was initiated. It was desired to know under what kind of weather conditions and over what kind of terrain type would coherent clutter processing be of value. The measurements were made using a step-scan phased array radar operating at a wavelength of 10 cm. The phased array antenna had a 4° horizontal and a 6° vertical beamwidth and the beam was steered parallel to the ground and swept through an 80° sector in 1° steps. At each pointing angle a single pulse of 1 μs duration was transmitted and the clutter returns recorded at a range bin spacing of 50 m. One sweep was made every 8 seconds with the beam step rate within the sweep being 1024 Hz. The peak power for the radar was 500 watts which limited the maximum useful range to 8 km.

A total of 50 sweeps were made each measurement day for a net recording time of 6.67 minutes. The returns were coherently demodulated, digitized at baseband, and recorded on digital magnetic tape. Along with the clutter data a sample of the transmitter pulse and a receiver calibration pulse were recorded to provide calibration information on a pulse-by-pulse basis. The local wind speed was also recorded.

A map of the area viewed by the radar is shown in Figure 7. The terrain to the left of the Ottawa River is mainly bushland and the terrain on the right is mainly urban and suburban. Four areas marked A, B, C and D areof special interest. Area A contains a small metal tower surrounded by bush, area B bush only, area C a combination of bush and rock, and area D an urban centre. Returns from each of these areas are discussed in detail.

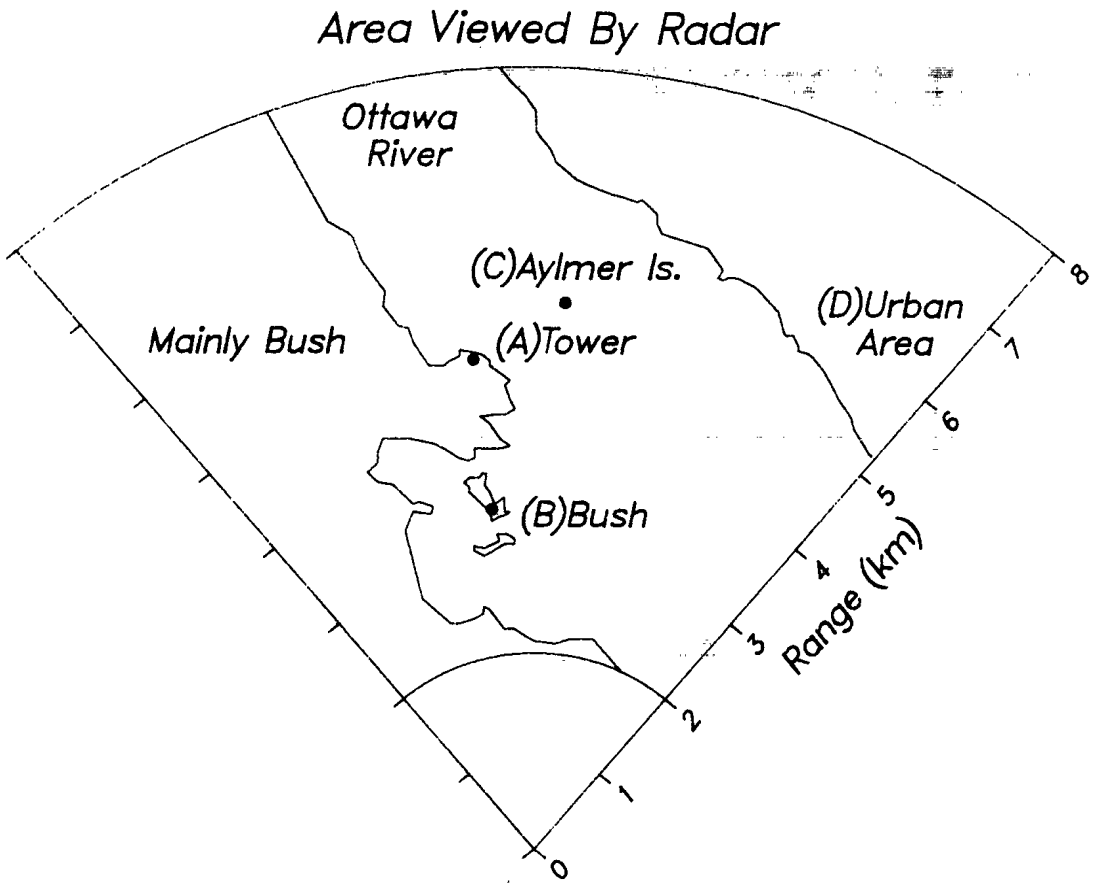

Fig. 7 Map of area view by the radar.

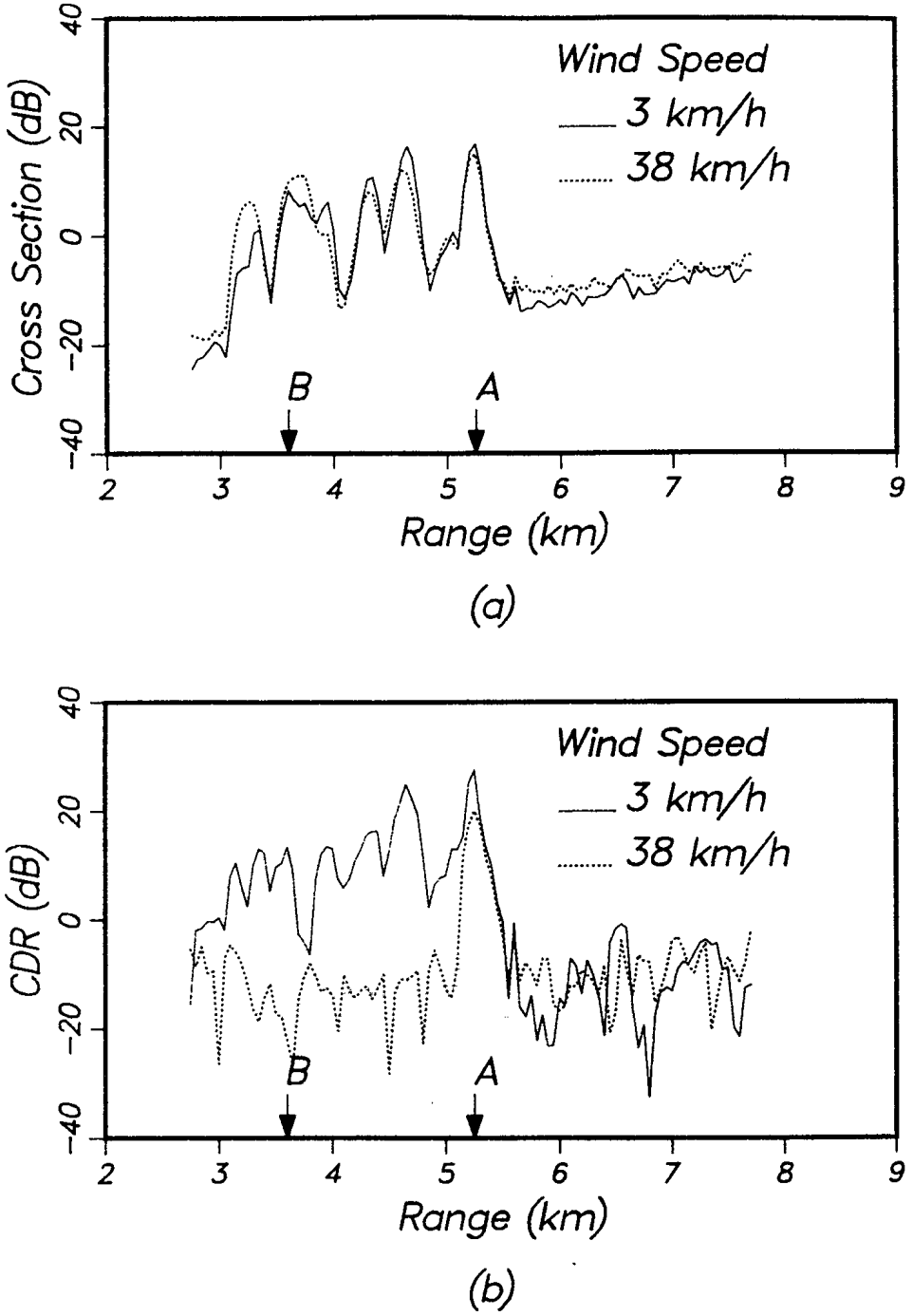

Fig. 8 Clutter returns from bushland for low and high wind speeds.

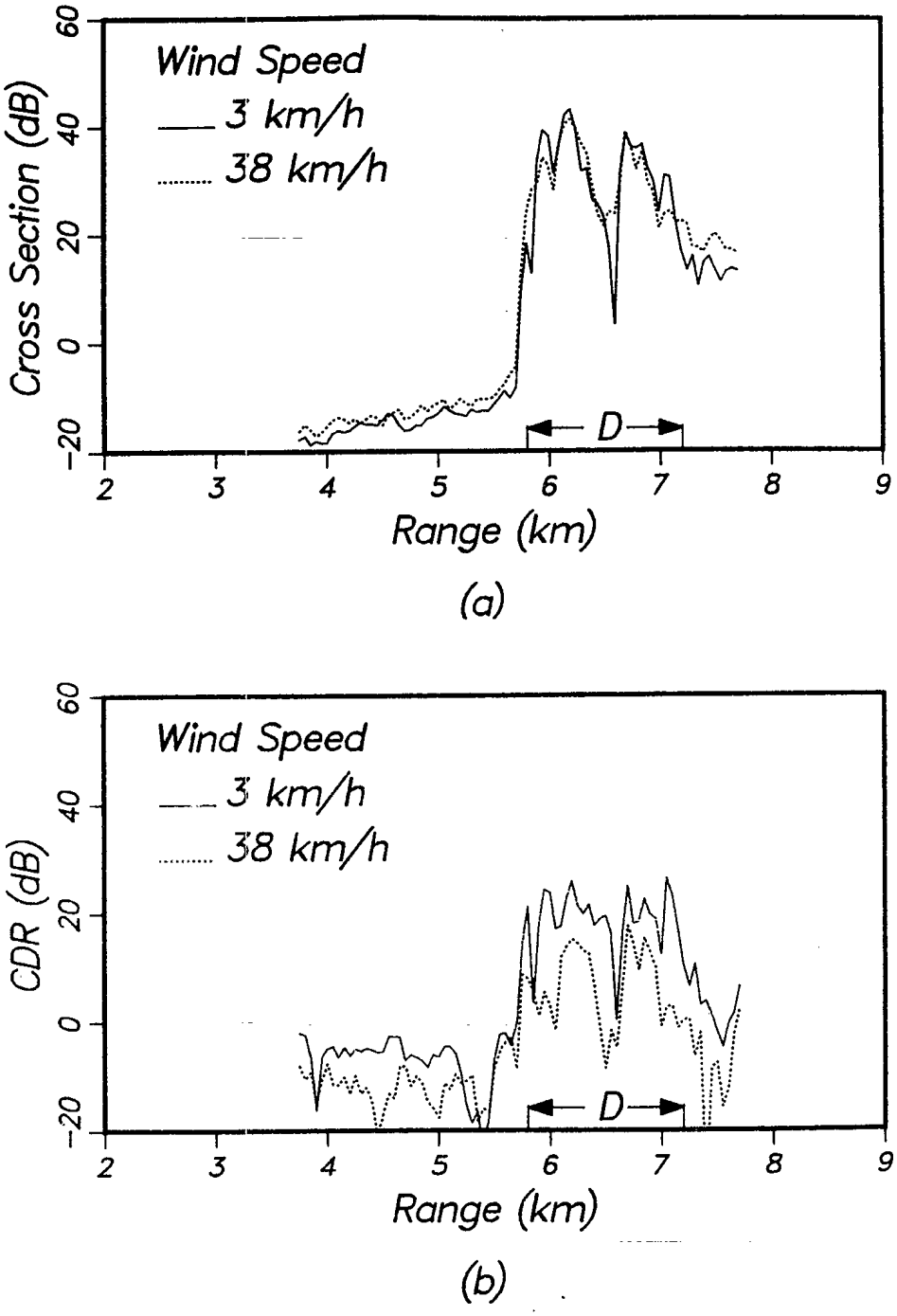

Fig. 9 Clutter returns from an urban centre for low and high wind speeds.

diffuse power with triangles and the CDR with squares. The straight line for each set of data points is marked at both ends with the appropriate symbol.

The first group (Figure 10a) was recorded for resolution cell B in Figure 7 and is typical of what was received for bushland in winter. For this type of terrain (leaveless trees and a snow cover) the CDR decreased for increasing wind speed with a slope of approximately -1.2 dB/km/h. This decrease was due to an increase in the diffuse component which was matched by a corresponding decrease in the coherent component. The total power however remained about the same. There is considerable spread about the straight line approximations for the total, diffuse, and coherent power but the points for the CDR fit reasonably well.

The second group (Figure 10b) was recorded for resolution cell C in Figure 7 and is typical of returns from a combination of rock, ice and trees. When these data were recorded the small rocky island was surrounded by ice and was covered with snow. For this type of terrain the CDR decreased with increasing wind speed with a slope of approximately -0.7 dB/km/h which is considerably less than the slope for cell B. The reason for the decrease is also different. In cell B both the diffuse and coherent components changed with wind speed but for cell C the coherent component remained fairly constant and the diffuse component alone changed. This indicates that a major portion of the clutter return from the island was from rock and ice whereas from the bushland it was from the trees. For this data set the straight lines are good approximations to the relationships with wind speed.

The third group (Figure 10c) was recorded for resolution cell A in Figure 7 and is typical of urban returns. This resolution cell contains a metal tower and some vegetation. Again the CDR decreased for increasing wind speed but the slope is only -.2 dB/km/h. The coherent power received and the total power were almost identical, with the diffuse power being about 25 dB lower for low wind speeds and 14 dB lower for high wind speeds. The decrease in CDR was due almost entirely to an increase in the diffuse component. For this group the data points were very tightly grouped around the straight line approximations.

Looking at the three winter condition groups together it can be seen that for low wind speeds all the terrain types exhibited a large coherent component that could be removed by coherent clutter processing. As the wind speed increased, however, the CDR decreased rapidly for the bushland, moderately for the combination of rock and bush and more slowly for the tower. It can be concluded that at high wind speeds coherent processing is valuable only in areas with little wind-induced motion such as urban centres.

Figure 11 shows measurements taken for the same resolution cells as above but under summer conditions (June 1984). The result for the bush (Figure 11a) is considerably different from that determined for winter (Figure 10a). The coherent component, although slightly smaller, behaves the same, decreasing with increasing wind speed, but the diffuse component

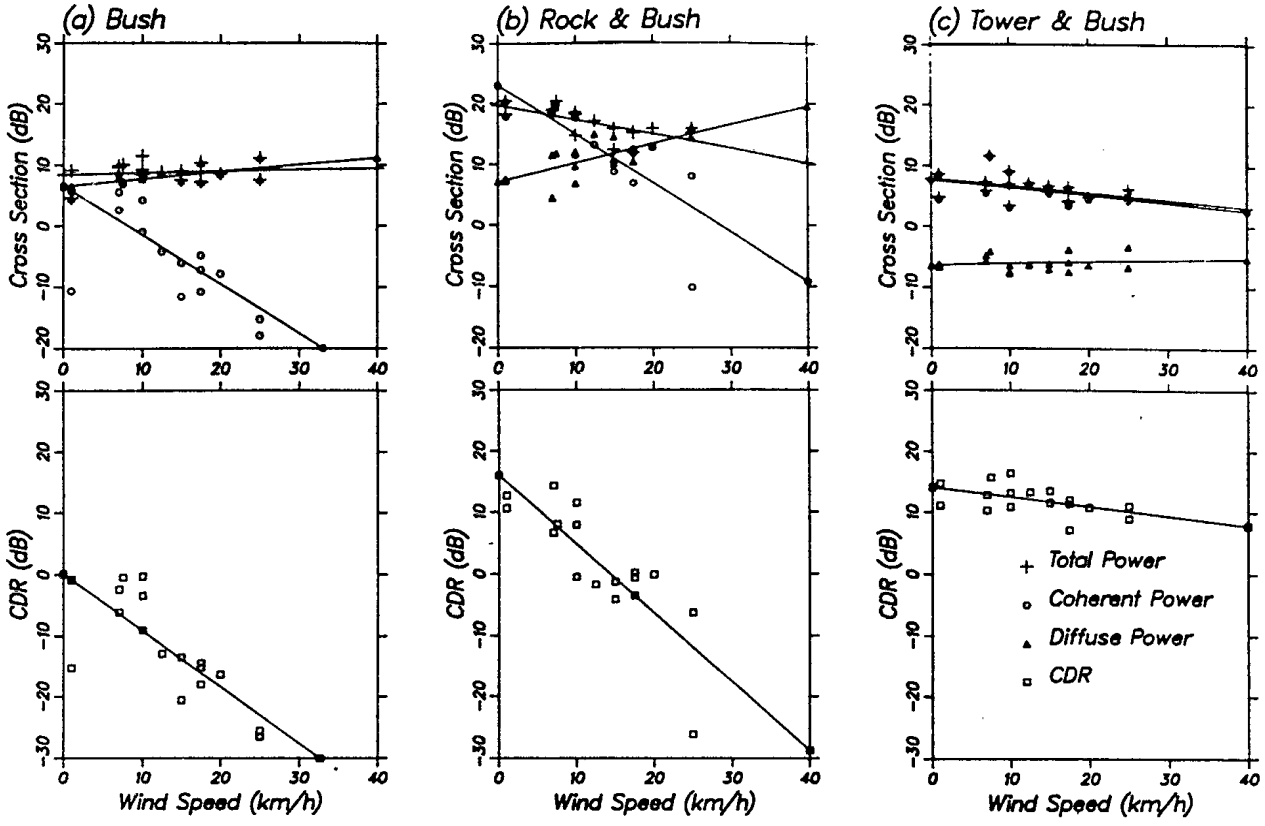

Fig. 11 Variations of returns with windspeed for three types of terrain under summer conditions.

remains relatively unaffected by the wind. Also the total return is almost entirely diffuse even at small wind speeds. The cause for this is that for trees with leaves the clutter returns are mainly diffuse even for the slightest of breeze and therefore an increasing wind speed does not add any additional randomness to the scatters. Coherent processing over summer bushland is therefore not an effective technique for clutter removal; however, for the identification of stationary structures its performance is enhanced because of the increased randomness of the background returns.

For the rock and bushland combination (Figure 11b) there is again a significant difference from the winter condition (Figure 10b). In the summer the complex clutter object behaves like winter bush terrain (Figure 10a). The coherent component decreases with increasing wind speed and the diffuse component increases. At low wind speeds coherent processing promises a gain of approximately 10 to 15 dB but this gain disappears rapidly once the wind speed reaches about 10 km/h.

For the tower and bush combination representing urban terrain the summer returns (Figure 11c) are not much different from the winter returns (Figure 10a) except in absolute level. This drop in level for the summer may be due to a partial shadowing of the tower by the leafy canopy of surrounding bush. The diffuse returns from the cell containing the tower do not increase significantly with wind speed as they did in the winter indicating that this component of the clutter may be saturated as mentioned above for the bush returns. The coherent component from the tower decreases slightly with increasing wind speed but at approximately the same slope as it did in the winter. The resulting CDR also decreases but is large enough (approximately 10 dB) to provide a significant gain with coherent processing.

The main difference between the winter and summer conditions is that the bush clutter in summer tends to be saturated with motion even at low wind speeds whereas in the winter it is not. This result indicates that coherent processing to remove clutter has merit in bush areas only in the winter and then only at low wind speeds. However in the summer it is still effective as a target identification procedure. In urban areas or areas that are similar (lack of vegetation) such as deserts or tundra coherent processing is valuable for both summer and winter and for both small and large wind speeds.

4.3 Daily Variations

It was shown earlier (Figure 2) that the coherent returns from a clutter object were stable in phase and amplitude over a period of about 7 minutes. Any processing scheme designed to take advantage of this stability must be able to adapt to slow variations that take place over larger time spans such as hours or days. To estimate these variations, radar returns from the radar range described by Figure 7 were recorded every 12 minutes for periods of up to 38 hours. Figure 12 shows the scatter plot for one 38 hour set of measurements for the range cell contaning the tower, and Figure 13 the time history of the phase of the

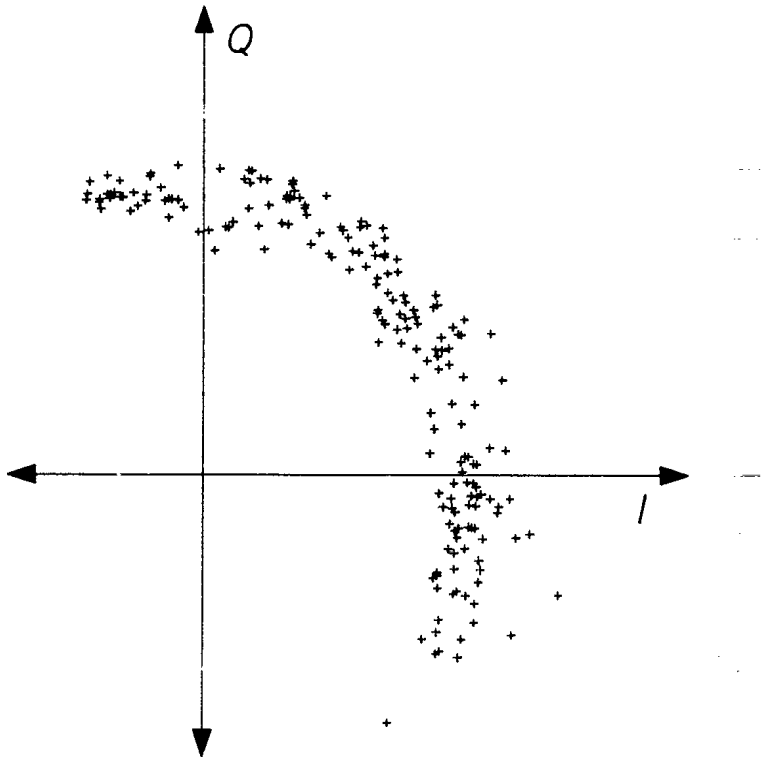

Fig. 12 Scatter plot of returns from the tower over a 38 hour time span.

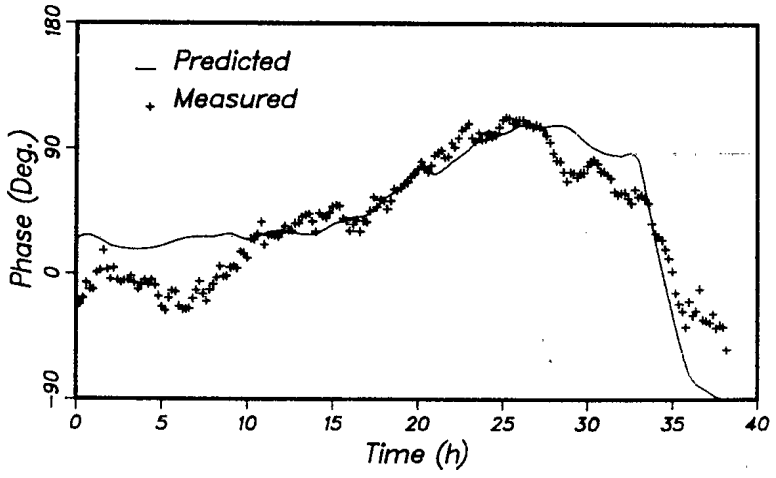

Fig. 13 Phase plot of returns from the tower over a 38 hour time span plus a prediction of the phase variation due to changes in temperature.

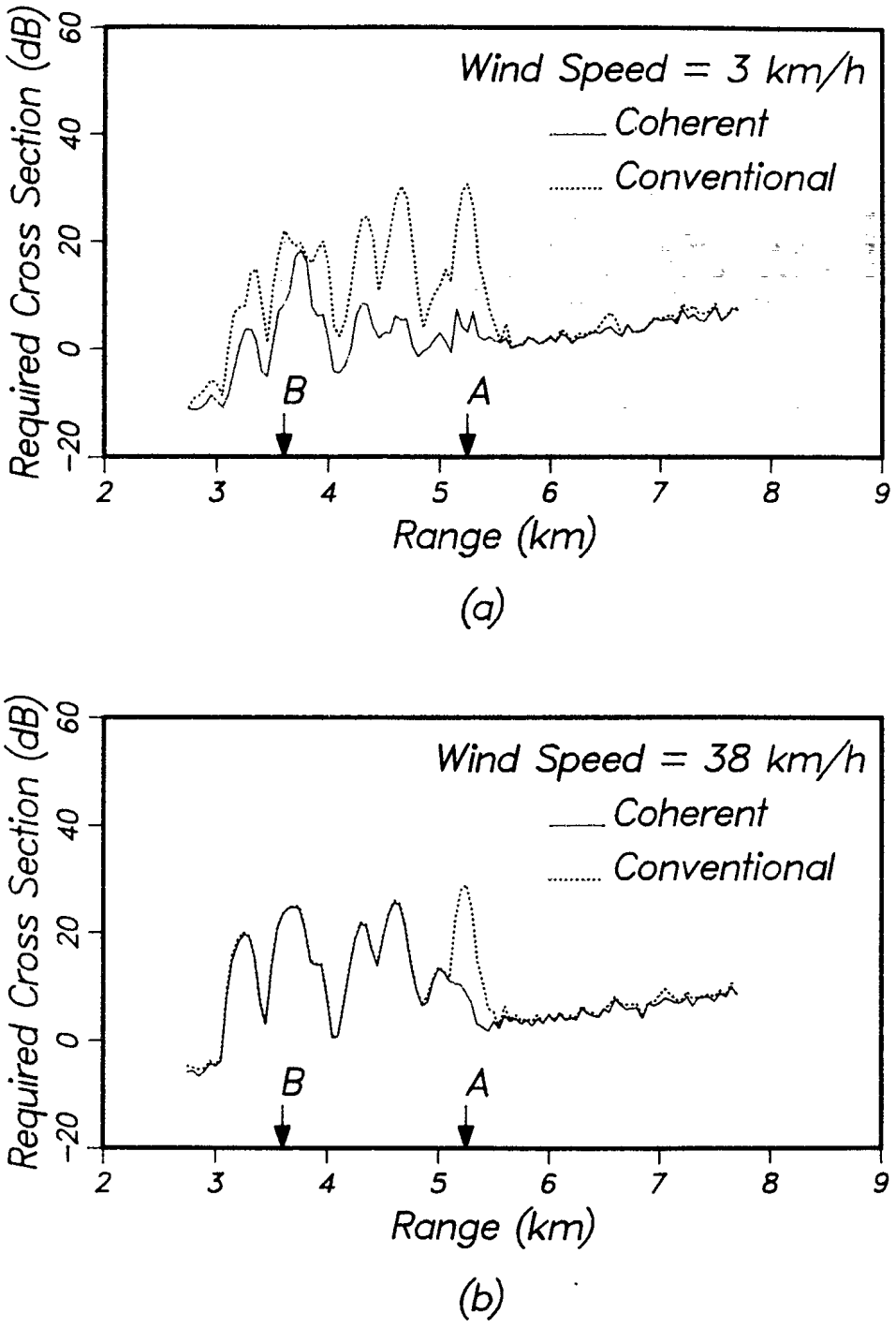

Fig. 14 Target cross section required for a single sample P_D of 0.8 and a P_F of 10^{-4} over bushland.

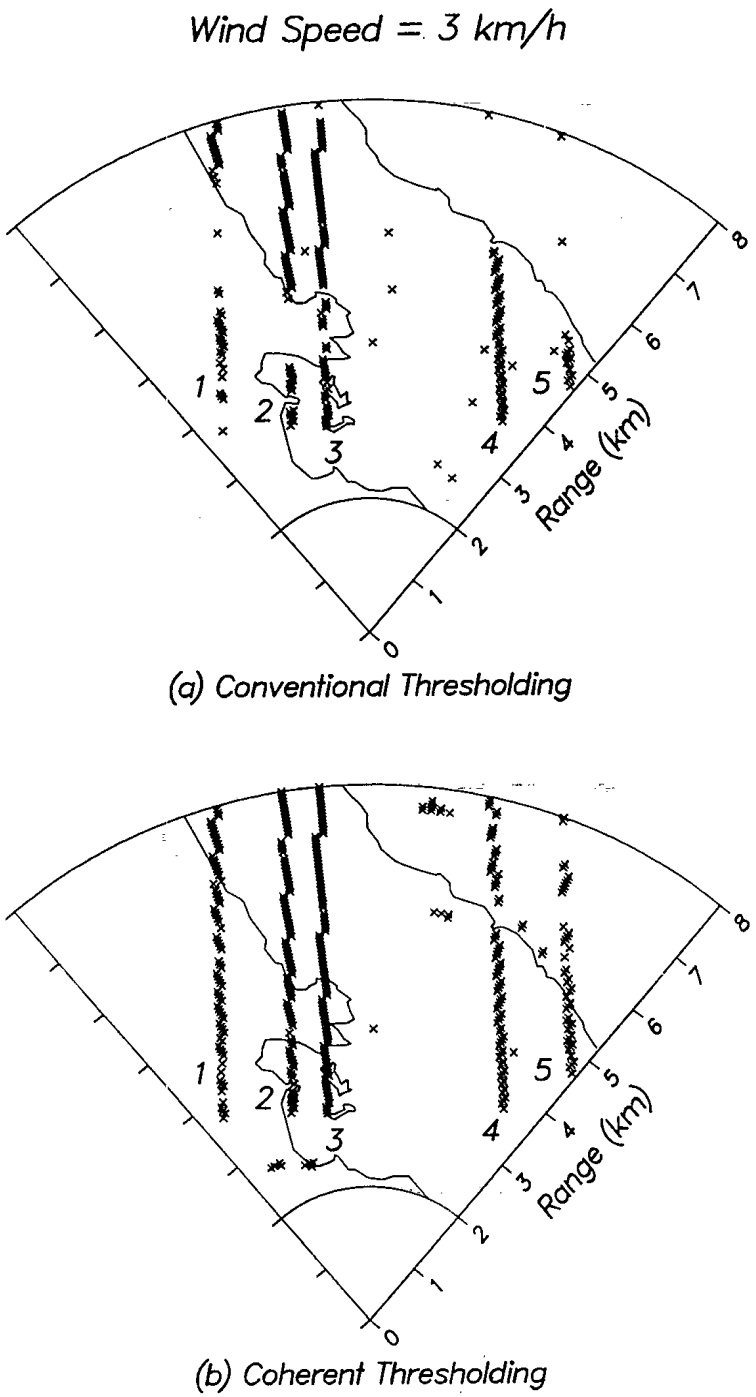

Fig. 16 Single sample tracks of simulated targets through real clutter for a low windspeed.

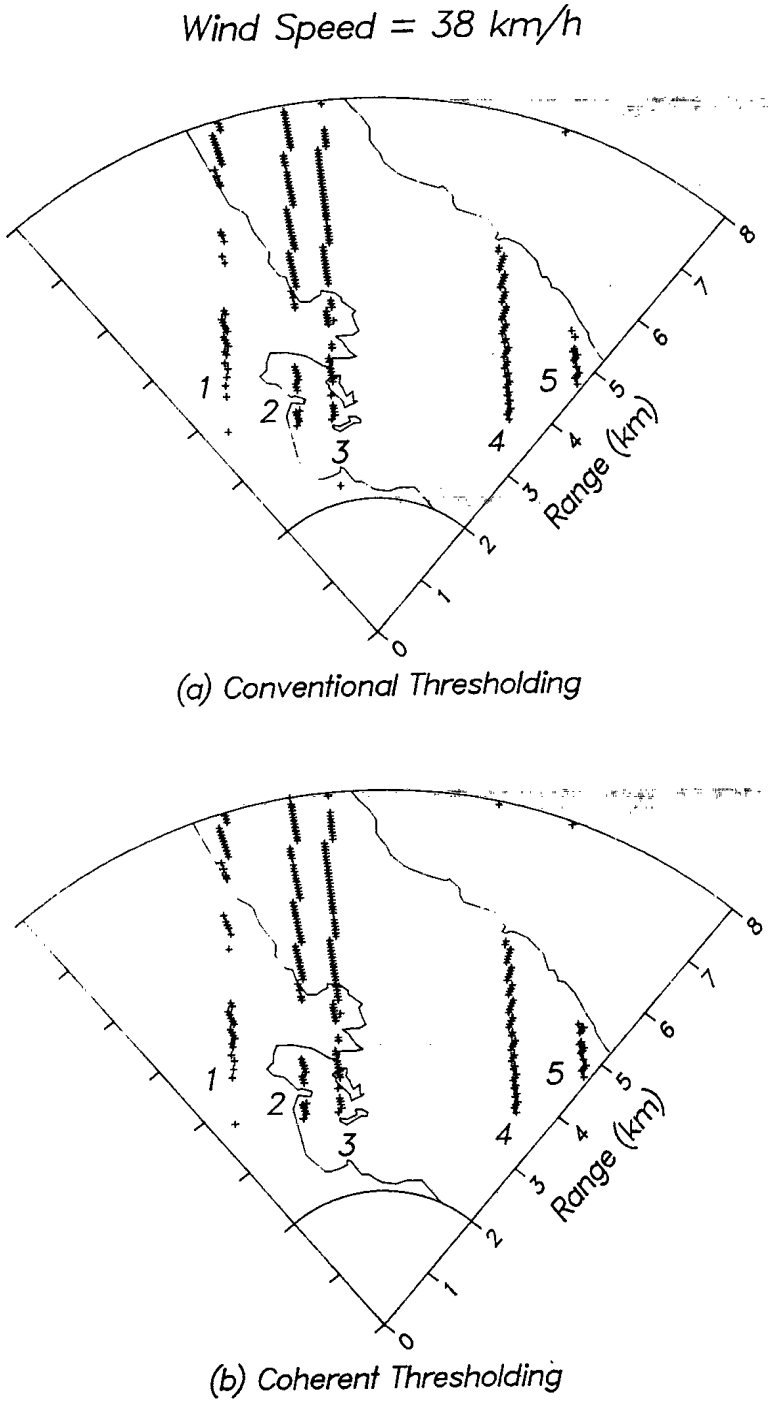

Fig. 17 Single sample tracks of simulated targets through real clutter for a high windspeed.

From these tracks it can be seen that coherent clutter processing has merit as a scheme to enhance low-Doppler target detection in high clutter areas.

6.0 CONCLUSION

In conclusion, this research into the coherent decomposition of clutter has resulted in some promising techniques that improve the detection and identification of low-Doppler targets. Experimental evidence supporting these techniques has been gathered using an S band phased array radar. Further work must be done to validate these techniques at higher frequencies where the motion induced by the wind is a larger fraction of the wavelength. Radars operating below S band should enjoy even greater gains than those described here.

APPENDIX

In this appendix it is shown that the gain in signal-to-interference ratio for using a coherent threshold, T_C, over another threshold, T, in order to obtain the same P_D is approximately equal to the ratio T^2/T_C^2 under the assumption of a large target signal. This gain is determined by equating the two expressions for P_D and solving for the resulting ratio of signal powers. Substituting bS^2+D^2 for S^2+D^2 in equation (14) and equating it to (17) we have

$$\exp\left(\frac{-T_C^2}{(S^2+D^2)}\right) = \int_T^\infty \frac{2r}{(bS^2+D^2)} \exp\left(\frac{-(C^2+r^2)}{(bS^2+D^2)}\right) I_0\left(\frac{2Cr}{(bS^2+D^2)}\right) dr \qquad \text{(A-1)}$$

where b is the ratio in signal powers required to make the equality hold. Since small argument approximations are to be used in the following it is convenient to change the limits of integraton to finite limits using the fact that $1-P_{DC}=1-P_D$. Therefore

$$1-\exp\left(\frac{-T_C^2}{(S^2+D^2)}\right) = \int_0^T \frac{2r}{(bS^2+D^2)} \exp\left(\frac{-(C^2+r^2)}{(bS^2+D^2)}\right) I_0\left(\frac{2Cr}{(bS^2+D^2)}\right) dr \qquad \text{(A-2)}$$

Under the assumption of a large S^2 the following small argument approximations are made

$$\exp(x) \simeq 1 + x \qquad \text{(A-3)}$$

$$I_0(x) \simeq 1 \qquad \text{(A-4)}$$

Therefore (A-2) becomes

$$\frac{T_C^2}{S^2+D^2} = \int_0^T \frac{2r}{bS^2+D^2}\left(1 - \frac{C^2}{bS^2+D^2} - \frac{r^2}{bS^2+D^2}\right) dr \qquad \text{(A-5)}$$

Performing the integration and rearranging terms we have

$$\frac{bS^2+D^2}{S^2+D^2} = \left(1-\frac{C^2}{bS^2+D^2}\right)\frac{T^2}{T_C^2} - \frac{1}{4(bS^2+D^2)}\frac{T^4}{T_C^4} \qquad \text{(A-6)}$$

In the limit as $S^2 \to \infty$ we have

$$b = \frac{T^2}{T_C^2} \qquad \text{(A-7)}$$

which is the required result.

REFERENCES

[1] Dax, P.R. (1975)
Eliminating Clutter in Radar Systems, Microwaves, (April 1975), page 34.

[2] Sutherland, J.W. (1977)
World Market Trends in Radar for Defence and Air Traffic Control, IEE Radar-77, (October 1977), 1-2.

[3] Meuhe, C.E., et al. (1974)
New Techniques Applied to Air-Traffic Control Radars, Proceedings of the IEEE, 62, 6 (June 1974), 716-723.

[4] O'Donnell, R.W., et al. (1974)
Advanced Signal Processing for Airport Surveillance Radars, EASCON '74, (1974), 71-71F.

[5] O'Donnel, R.M. and Muehe, C.E. (1979)
Automatic Tracking for Aircraft Surveillance Radar Systems, IEEE Transaction on Aerospace and Electronic Systems, AES-15, 4 (July 1979), 508-517.

[6] Bird, J.S. (1982)
Ground Clutter Suppression Using a Coherent Clutter Map, IEE Radar '82 (October 1982), 491-495.

[7] Bird, J.S. (1984)
Subclutter Visibility for Low-Doppler Targets, IEEE ISNCR'84, Tokyo, Japan (October 1984), 47-52.

[8] Parl, S. (1980)
A New Method of Calculating the Generalized Q Function, IEEE Transactions on Information Theory, IT-26, 1 (January 1980), 121-124.

[9] Skolnik, M.I. (1962)
Introduction to Radar Systems, McGraw-Hill, 1962, page 506.

UNCLASSIFIED

Security Classification

KEY WORDS

Low-Doppler
Detection
Clutter

INSTRUCTIONS

1. ORIGINATING ACTIVITY: Enter the name and address of the organization issuing the document.

2a. DOCUMENT SECURITY CLASSIFICATION: Enter the overall security classification of the document including special warning terms whenever applicable.

2b. GROUP: Enter security reclassification group number. The three groups are defined in Appendix 'M' of the DRB Security Regulations.

3. DOCUMENT TITLE: Enter the complete document title in all capital letters. Titles in all cases should be unclassified. If a sufficiently descriptive title cannot be selected without classification, show title classification with the usual one-capital-letter abbreviation in parentheses immediately following the title.

4. DESCRIPTIVE NOTES: Enter the category of document, e.g. technical report, technical note or technical letter. If appropriate, enter the type of document, e.g. interim, progress, summary, annual or final. Give the inclusive dates when a specific reporting period is covered.

5. AUTHOR(S): Enter the name(s) of author(s) as shown on or in the document. Enter last name, first name, middle initial. If military, show rank. The name of the principal author is an absolute minimum requirement.

6. DOCUMENT DATE: Enter the date (month, year) of Establishment approval for publication of the document.

7a. TOTAL NUMBER OF PAGES: The total page count should follow normal pagination procedures, i.e., enter the number of pages containing information.

7b. NUMBER OF REFERENCES: Enter the total number of references cited in the document.

8a. PROJECT OR GRANT NUMBER: If appropriate, enter the applicable research and development project or grant number under which the document was written.

8b. CONTRACT NUMBER: If appropriate, enter the applicable number under which the document was written.

9a. ORIGINATOR'S DOCUMENT NUMBER(S): Enter the official document number by which the document will be identified and controlled by the originating activity. This number must be unique to this document.

9b. OTHER DOCUMENT NUMBER(S): If the document has been assigned any other document numbers (either by the originator or by the sponsor), also enter this number(s).

10. DISTRIBUTION STATEMENT: Enter any limitations on further dissemination of the document, other than those imposed by security classification, using standard statements such as:

(1) "Qualified requesters may obtain copies of this document from their defence documentation center."

(2) "Announcement and dissemination of this document is not authorized without prior approval from originating activity."

11. SUPPLEMENTARY NOTES: Use for additional explanatory notes.

12. SPONSORING ACTIVITY: Enter the name of the departmental project office or laboratory sponsoring the research and development. Include address.

13. ABSTRACT: Enter an abstract giving a brief and factual summary of the document, even though it may also appear elsewhere in the body of the document itself. It is highly desirable that the abstract of classified documents be unclassified. Each paragraph of the abstract shall end with an indication of the security classification of the information in the paragraph (unless the document itself is unclassified) represented as (TS), (S), (C), (R), or (U).

The length of the abstract should be limited to 20 single-spaced standard typewritten lines; 7½ inches long.

14. KEY WORDS: Key words are technically meaningful terms or short phrases that characterize a document and could be helpful in cataloging the document. Key words should be selected so that no security classification is required. Identifiers, such as equipment model designation, trade name, military project code name, geographic location, may be used as key words but will be followed by an indication of technical context.

#49783

8801a	1	Copy #	1
b	DAG	Information Scientist	
8802a	DRED		
b			
c			
8803	FEB FEV 18 1987	90	
DSIS ACCN#	87-00940		

DIRECTOR SCIENTIFIC
INFORMATION SERVICES
NATIONAL DEFENCE HEADQUARTERS
OTTAWA, ONTARIO
K1A 0K2

FEB FEV 26 1987